Published in final edited form as:
Biol Cybern. 2005 November ; 93(5): 309–322.

Feedback equilibrium control during human standing

Alexei V. Alexandrov and **Frolov AA**
Institute of Higher Nervous Activity and Neurophysiology, Russian Academy of Science Butlerova 5a, Moscow 117485, Russia, Tel: (095) 334-4345, Fax: (095) 338-8500; E-mail: alexeialexandrov@inbox.ru

Horak FB, **Carlson-Kuhta P**, and **Park S**
Oregon Health and Science University, Portland, OR, USA

Abstract

Equilibrium maintenance during standing in humans was investigated with a 3-joint (ankle, knee and hip) sagittal model of body movement. The experimental paradigm consisted of sudden perturbations of humans in quiet stance by backward displacements of the support platform. Data analysis was performed using eigenvectors of motion equation. The results supported three conclusions. First, independent feedback control of movements along eigenvectors (eigenmovements) can adequately describe human postural responses to stance perturbations. This conclusion is consistent with previous observations (Alexandrov et al., 2001b) that these same eigenmovements are also independently controlled in a feed-forward manner during voluntary upper-trunk bending. Second, independent feedback control of each eigenmovement is sufficient to provide its stability. Third, the feedback loop in each eigenmovement can be modeled as a linear visco-elastic spring with delay. Visco-elastic parameters and time-delay values result from the combined contribution of passive visco-elastic mechanisms and sensory systems of different modalities.

1 Introduction

For maintaining upright human posture during stance, the large mass of the upper trunk and its elevated position over the small support base complicates the control of equilibrium. A controversy among investigators of orthograde posture is whether the central nervous system (CNS) controls balance in a feedback manner, generating corrective muscle forces as automatic responses to equilibrium disturbances, as suggested by Peterka (2002) and others, or whether feed forward anticipatory corrections are also required to provide upright standing (Fitzpatrick et al. 1996).

Two main factors determine muscle forces: first, the reference equilibrium body configuration and second, the deflexion of actual body configuration from this reference. The automatic involuntary change of muscle forces in response to *deflexions from a given reference* is the essence of the *feedback* control. The *change of parameters of the feedback control* (of the equilibrium body configuration and of the feedback loop gains) is the essence of the *feed forward* control that can be performed either voluntary or involuntary. In motor control theory, the feedback loop and the controlled plant constitute an autonomous “closed-loop” system, while the feed forward control provides external input signals to this system in the “open-loop” manner. We emphasize that feed forward control implies the control of parameters of the feedback loop but not direct control of muscle forces (Feldman and Ostry 2003).

A voluntary trunk bend in standing humans, which is caused by a change of the equilibrium body configuration, is an example of voluntary feed forward control. The anticipatory body inclination in a standing passenger before the start of a train is an example of involuntary feed forward corrections. Such anticipatory corrections are possible only when the forthcoming perturbations are predictable, for example, when they are preceded by a relevant signal or are

correlated in time (Gurfinkel et al. 1995; Fitzpatrick et al. 1996). The experimental protocol used in the present study was aimed to minimize the predictability of perturbations: first, the quietly standing subjects were imposed to *sudden* support platform shifts of *random* amplitudes; second, only relatively short early phase of responses were analyzed (up to 1.3 s after the perturbation onset). The study of Gurfinkel et al. (1995), suggests that the characteristic time for adjustment of the feedback loop parameters during orthograde posture is about 10 s. Therefore, during the short, early phase of the response feed forward control is likely small and posture maintenance is determined mainly by the feedback mechanisms. The goal of the present study was to investigate parameters of these mechanisms and, thus, to bring into light the controversy about whether feedback control is sufficient to provide balance stability in unrestrained standing human.

The continuous feedback loop is taken in the form of a linear visco-elastic spring (Barin 1989; Morasso and Schieppati 1999; Winter et al. 1998, 2001; Park et al. 2004) with time delays (Peterka 2002). The gain coefficients that determine dependence of torques on joint angles and angular velocities are called stiffness and viscosity coefficients respectively.

In analyses of balance stability in humans, the body is usually represented as a one-dimensional inverted pendulum rotating about the ankle joints (Morasso and Schieppati 1999; Winter et al. 2001; Kiemel et al. 2002; Peterka 2002; Micheau et al. 2003). In such a model, the biomechanical system is described by only one variable: the angle of the ankle joint. In this one-dimensional model, only torque at the ankle joint corrects body sway. The attractiveness of a one-dimensional model is that it allows for simple measurements of both the controlled (ankle joint angle) and controlling (ankle joint torque) variables.

However, the human body as a biomechanical system can be more accurately modeled by a multi-joint chain. In such a model, due to the interaction among links in the chain, the change of torque in any joint influences on the movement in all the joints. Therefore, the validity of the one-dimensional model for the analysis of balance control seems doubtful. Such an approach may be valid only if the movements in all the joints, except the ankle, are artificially blocked (Peterka 2002).

The properties of the feedback loop that controls the equilibrium of the body as a multi-joint biomechanical system are described in our previous study (Park et al. 2004) in the frame of full-state feedback control which implies that each joint torque depends on all the joint angles (Barin 1989). The present study goes further and claims that coefficients of the stiffness and viscosity matrices of the full-state control model are not independent and thus this model is overparameterized. To reveal the nature of this overparametrisation, the present study exploits the approach previously developed for the analysis of voluntary bending of the human upper trunk in the sagittal plane (Alexandrov et al. 2001a). In this approach, movement is described in terms of eigenvectors of a motion equation. By definition of eigenvectors (see below), the movement along each eigenvector (eigenmovement) is characterized by the linear relationship between joint angles and simultaneously linear relationship between joint torques.

An eigenmovement is named according to the joint that dominates the respective eigenmovement (Fig. 1). For a three-joint model of the human body, there are three, “Ankle” (A), “Hip” (H) and “Knee” (K), eigenmovements. As schematically illustrated in Fig. 1, any movement of the human body in the sagittal plane can be represented as a superimposition of eigenmovements with different kinematical amplitudes. Formally, the kinematic amplitude of each eigenmovement is a generalized coordinate in joint angle space. The matrix of transformation from joint angles to these generalized coordinates is given by equation (4), see below. Similarly, the joint torques in any movement can be represented as a superimposition of joint torques in eigenmovements with different dynamic amplitudes. The

dynamic amplitude of each eigenmovement is a generalized force in the joint torque space. The matrix of transformation from joint torques to these generalized forces is given by equation (6), see below.

The convenience of transition from the usual description of movement dynamics and kinematics in terms of joint torques and angles to these generalized forces and coordinates is that each eigenmovement is described by the simple motion equation as for a one-dimensional inverted pendulum. As shown by Alexandrov et al. (2001a), the inertia among the three "eigenmovement pendula" essentially differs (the ratio is 50:10:1, for A-, H-, and K-eigenmovements, respectively). These differences in inertia require different temporal organization of control signals for each separate eigenmovement (different feedback delays, durations of the signals, their onset and offset times and time profiles). Therefore, the separate independent control of each eigenmovement according to its specific inertia could simplify the control of the whole multijoint biomechanical system. The unique inertia, along with the simple kinematics (fixed ratios between joint angles, i.e. "kinematical synergy") and dynamics (fixed ratios between joint torques, i.e. "dynamical synergy") of eigenmovement supports the hypothesis that it might be controlled by one command distributed among all joints with different fixed weights (i.e. "synergy of control signals"). Therefore, eigenmovements can be regarded as some specific "natural synergies" defined by human body anthropometric properties. The control of any movement might be organized by the CNS in the form of proper coordination of eigenmovements as entire control units. This suggestion was supported in experiments in which humans voluntarily bent the upper trunk while standing on a flat support surface and on a narrow beam (Alexandrov et al. 2001b). Under both conditions, the most inertial A-eigenmovement started earlier and terminated later than less inertial H-eigenmovement. The change in support size resulted only in changes in eigenmovements'amplitudes, without a change in the time profile of an individual eigenmovement. The results of our previous study (Alexandrov et al. 2004) are in favor with the suggestion that eigenmovements are independently controlled not only in a feed forward manner as found during voluntary trunk bending but also in a feedback manner. The time delay in the feedback loop of each eigenmovement actually appeared to be adjusted to its inertia: the larger the inertia, the larger the delay.

The independent control of each eigenmovement implies that "stiffness" and "viscosity" matrices in terms of eigenmovements are diagonal, i.e. the generalized force (dynamic amplitude) in each eigenmovement is completely determined by the generalized coordinate (kinematical amplitude) of this eigenmovement. However, the transformation from these generalized coordinates and forces to the usual joint angles and torques, see equation (15) below, results in non diagonal stiffness and viscosity matrices. In this sense, the eigenmovement approach is a special case of the full-state control approach. The present study claims that coefficients of stiffness and viscosity matrices in terms of joint torques and angles are tuned to provide the diagonality of the similar matrices in terms of eigenmovements. Thus, 6 parameters (3 stiffness and 3 viscosity coefficients) in the proposed independent eigenmovement control completely determine 18 parameters (3 x 3 stiffness and 3 x 3 viscosity matrices) in the full-state feedback approach. Thus, we consider that diagonality of stiffness and viscosity matrices in terms of eigenmovements is the nature of the overparametrisation of the full-state approach.

2 Methods

2.1 Experimental protocol

Nine humans, aged 20 to 32 years and with no history or evidence of orthopedic, muscular, or neurological motor disorders, were tested. Subjects gave informed consent prior to data

collection, in accordance with the regulations and standards governed by the Institutional Review Board of Oregon Health & Science University's Office of Research Integrity.

Subjects stood quietly on a support platform, with arms by their sides and looking straight ahead. They were instructed to keep their balance in response to any sudden movements of the platform and to avoid stepping or lifting their heels off the ground, if possible. The support platform shifted backward with ramp displacements of 275 ms in duration. The displacement amplitudes (also termed *perturbation amplitudes*) were 3, 4.5, 6, and 7.5 cm. The perturbation amplitudes were large enough to provoke body sway that is known to exceed natural sway (Winter et al. 2001). On the other hand, the amplitudes were small enough to avoid nonlinear effects in the motion equation.

For each trial, kinematics and ground reaction-force data were recorded. The time interval analyzed was 1400 ms –50 ms prior to and 1350 ms after the onset of a perturbation. The relatively short period of analysis minimized the probability of voluntary feed-forward corrections, which could disturb estimations of the feedback loop parameters. It is doubtful that feed-forward corrections are absent during longer time periods, for example 6 s, as used in Barin (1989).

Kinematic data were recorded at a sampling rate of 120 Hz, using an optical system with 6 cameras (Motion Analysis Corp., Santa Rosa, CA). One optical marker was attached to the platform surface, and four markers were placed on the right side of the subject's right ankle (lateral malleolus), knee (lateral femoral condyle), hip (greater trochanter), and shoulder (acromiom). The marker positions were used to calculate the length of body segments and joint angles.

Ground reaction forces and the ankle joint torques for each leg were recorded at a sampling rate of 480 Hz from force transducers located in the support platform.

All data were averaged across all trials of the same perturbation amplitude for each subject. These averaged data were processed by standard statistical methods.

2.2 Data analysis

2.2.1 Eigenmovement approach—Human dynamics in the sagittal plane were represented as a three-link inverted pendulum (Barin 1989; Yang et al. 1990; Kuo and Zajac 1993; Fig.1, top). Body segments were assumed to be thin rigid links rotating around three ideal pin joints (hip, ankle and knee), with a torque actuator at each pin joint.

The motion equation of a three-rigid-link system under gravity and a platform perturbation is:

$$\boldsymbol{C}(\boldsymbol{\varphi})\ddot{\boldsymbol{\varphi}} - \boldsymbol{D}(\boldsymbol{\varphi})\boldsymbol{\varphi} + \boldsymbol{A}(\boldsymbol{\varphi}, \dot{\boldsymbol{\varphi}}) = \boldsymbol{T} + \boldsymbol{P}(\boldsymbol{\varphi})a_x, \quad (1)$$

where $\boldsymbol{\varphi}$ is the vector of hip, knee, and ankle joint angles, **T** is the vector of internal joint torques produced by muscles, $\mathbf{P}a_x$ is the vector of external torques produced by the platform movement ("perturbation"), and a_x is the horizontal acceleration of the axis of rotation. In vectors $\boldsymbol{\varphi}$, **T**, and **P**, the first, second and third components relate to the ankle, knee, and hip, respectively. **C** and **D** are inertial and gravitational matrices, and vector **A** defines centripetal and Coriolis forces.

The elements of matrices **C** and **D** and the components of vectors **A** and **P** were calculated using standard anthropometric tables (Winter 1990), taking into account each subject's weight, height, and length of segments (Appendix A).

In the present study, we used the linear approximation of (1), which has the form

$$C\ddot{\varphi} - D\varphi = T + Pa_x, \tag{2}$$

where, in contrast to (1), the inertial matrix **C** and gravitational matrix **D** are angle-independent (Appendix A). In the present experiments, the difference between joint torques calculated by (1) and (2) did not exceed 3% of torque variance in each joint.

The linear approach allowed us to decompose the three joint movements of subjects into three components ("eigenmovements"), with each component representing a movement along one of the three eigenvectors $\mathbf{w}_i$ in the linear motion equation (2). The eigenvectors are defined by

$$D^{-1}Cw_i = \lambda_i w_i, \tag{3}$$

where λ_i are corresponding eigenvalues, **C** and **D** are inertial and gravitational matrices from equation (2). The subscript ($i = A,H,K$) corresponds to the dominant component in each eigenvector (see Fig. 1).

The presentation of the joint movements in terms of eigenmovements implies the transformation of the joint-angle vector $\boldsymbol{\phi}(t)$ into the vector $\boldsymbol{\xi}(t)$ of eigenmovement "kinematic scaling amplitudes" by an inversion of the equation:

$$\varphi(t) = W\xi(t), \tag{4}$$

where columns of matrix **W** are eigenvectors $\mathbf{w}_i$ and each component of vector $\boldsymbol{\xi}(t)$ defines the time course of the movement along each eigenvector (eigenmovement).

The "dynamic scaling amplitudes" η_i and χ_i for internal and external torques of each eigenmovement were calculated by inserting (4) into (2). Taking into account (3), we obtained three independent, dynamic equations for each eigenmovement

$$-\lambda_i\xi_i + \xi_i = \eta_i + \chi_i a_x, \tag{5}$$

where the vectors of dynamic scaling amplitudes $\boldsymbol{\eta}$ and $\boldsymbol{\chi}$ are

$$\eta(t) = U^{-1}T(t), \quad \chi(t) = U^{-1}P(t), \tag{6}$$

and the matrix

$$U = -DW \tag{7}$$

defines the contribution of each eigenmovement to the total joint torques.

The advantage of analyzing the motion equation in terms of eigenmovements is the splitting of the coupled vector dynamic equation (2) into three simple, independent, scalar motion equations (5). As shown in Appendix B, in the system of coordinates bounded to the moving platform,

$$X_i^{\mathrm{CG}} = b_i\xi_i, \quad X_i^{\mathrm{CP}} = b_i\eta_i, \tag{8}$$

and the relationship between the center of gravity (CG) X^{CG}_i and the center of pressure (CP) X^{CP}_i in each i-th eigenmovement takes a simple form

$$-\lambda_i \ddot{X}_i^{CG} + X_i^{CG} = X_i^{CP} - b_i \chi_i a_x(t), \tag{9}$$

where the coefficients b_i are defined by human anthropometric parameters (Appendix B). The total CP and CG displacements are the sums of corresponding displacements in each eigenmovement.

For example, for a *standard human* of 70 kg body mass, 170 cm height, and standardized anthropometric parameters of the body segments (Winter 1990), (3) gives the following eigenvalues for A-, H-, and K-eigenmovements:

$$\lambda_A = 0.108\,\mathrm{s}^2, \quad \lambda_H = 0.020\,\mathrm{s}^2, \quad \lambda_K = 0.0021\,\mathrm{s}^2. \tag{10}$$

The contribution of each joint angle and joint torque to each eigenmovement for this *standard human* is illustrated in Fig. 1, in which eigenmovements are ordered from left to right by the decreasing eigenvalue λ_i(i.e., *eigenmovement inertia*).

The coefficients χ_i and b_i ($i = A,K,H$) in (5) and (8) for the *standard human* are the following:

$$\begin{aligned} &\chi_A = 9.4 \times 10^{-2}\,\mathrm{s}^2\,\mathrm{rad/m}, \quad \chi_H = 3.3 \times 10^{-2}\,\mathrm{s}^2\,\mathrm{rad/m}, \\ &\chi_K = 8.5 \times 10^{-3}\,\mathrm{s}^2\,\mathrm{rad/m} \\ &b_A = 9.3 \times 10^{-3}\,\mathrm{m/rad}, \quad b_H = 4.5 \times 10^{-4}\,\mathrm{m/rad}, \\ &b_K = 8.5 \times 10^{-5}\,\mathrm{m/rad} \end{aligned} \tag{11}$$

The kinematic pattern of A-eigenmovement (given by eigenvector $\mathbf{w}_A$) is similar to whole-body rotation around the ankle joint (Fig. 1, left). Ankle-joint flexion, accompanied by hip flexion and knee extension, results in a forward CG shift. The kinematic pattern of H-eigenmovement ($\mathbf{w}_H$) is similar to forward trunk bending, which is accompanied by opposite displacements of upper and lower body segments (Fig. 1, middle). Despite the forward trunk bend due to hip flexion, CG in the H-eigenmovement shifts backward due to the contribution of the ankle extension. The kinematic pattern of K-eigenmovement ($\mathbf{w}_K$) is similar to the sitting down movement performed by knee flexion and vertical translational movement of the trunk segment (Fig. 1, right).

Torque at each of the ankle, knee, and hip joints was calculated by (2) using kinematic recordings. At that, the calculations of the 2nd derivatives of joint angles was performed using Savitzky-Goley parabolic filter with 7-points running window (Orfandis 1996). According to this procedure, the best fitted parabola is curved through the seven adjacent experimental points. The value of the fitted curve at the middle point is treated as the filtered value at this point, and the 2nd derivative of the parabola is treated as the filtered value of the 2nd derivative at the middle point. The accuracy of torques calculations by the kinematic data was estimated by the comparison between the calculated ankle joint torque and its value directly measured by the force platform. Fig. 2 shows the typical result of the performed calculations. Across all subjects and trials, the mean square difference between two curves ranged from 2 to 4% of the ankle joint torque excursion.

Kinematic amplitudes $\xi_i(t)$ were calculated by the inversion of (4), and dynamic amplitudes $\eta_i(t)$ were calculated by (6) in which the ankle joint torque was directly measured by the platform and the hip and knee joint torques were calculated by the kinematical data. The time course of variables $X^{CG}{}_i(t)$ and $X^{CP}{}_i(t)$ that define the contributions of each eigenmovement into the total CG and CP displacements were calculated by (6) and (8).

2.2.2 Model of feedback control—The feedback control system transforms the current joint angles into the corrective joint torques. Different models for such transformations have been considered previously. For the control of balance, the most detailed models take into account the peculiarities of contributions from different sensory systems (visual, vestibular, proprioceptive, and tactile) (for review see Horak and Macpherson 1996). This complex approach requires a complicated description of sensory-motor transformations during posture stabilization (van der Kooij et al. 1999, 2001; Kiemel et al. 2002). The simplest description of the feedback loop is its approximation by a visco-elastic linear spring-like model (Barin 1989; Morasso and Schieppati 1999; Winter et al. 1998, 2001; Park et al. 2004). The reasonable compromise between these two extreme approaches is the linear visco-elastic spring-like model with a superposition of two feedback loops: with and without time delay (Peterka 2002). They were referred by Peterka as “active” and “passive” feedbacks. However, the “passive” stiffness and viscosity appeared to be in order less than the “active” ones and the separation of the passive feedback loop did not increase significantly the accuracy of the feedback model (Peterka 2002). Taking into account this result, we ignored the passive loop without delay and used only feedback loop with delay being aware that such delay reflects some “effective” value and is a result of performance of several feedback mechanisms with and without delays (see Discussion).

In the present study, the principal peculiarity of the used model of the feedback control is the suggestion that each eigenmovement is independently controlled by its own feedback loop. In terms of eigenmovements, corrective joint torques are given by $\boldsymbol{\eta}$ and joint angles by $\boldsymbol{\xi}$. Then, according to our principal suggestion, the corrective dynamic amplitude η_i in each eigenmovement is completely determined by the kinematic amplitude *only* in this eigenmovement. In this case, the feedback loop for each eigenmovement is described as

$$\eta_i(t) = K_i^S(\xi_i(t-\tau_i) - \xi_{0i}) + K_i^V \xi_i(t-\tau_i) \qquad i = A,\ H,\ K, \tag{12}$$

or, taking into account (8), the feedback loop is

$$X_i^{\mathrm{CP}}(t) = K_i^S(X_i^{\mathrm{CG}}(t-\tau_i) - X_{0i}^{\mathrm{CG}}) + K_i^V X^{\mathrm{CG}}(t-\tau_i), \qquad i = A,\ H,\ K, \tag{13}$$

where K^S_i and K^V_i are *stiffness* and *viscosity*, respectively, in terms of eigenmovements; τ_i is the delay; and ξ_{0i} determines the body posture that is comfortable for quiet standing.

If we ignore time delays τ_i in the feedback control loops, then (12) can be rewritten in the conventional form of full-state feedback model:

$$\boldsymbol{T}(t) = -\boldsymbol{S}(\boldsymbol{\varphi}(t) - \boldsymbol{\varphi}_0) - \boldsymbol{V}\dot{\boldsymbol{\varphi}}(t), \tag{14}$$

where $\boldsymbol{\phi}_0$ determines the equilibrium body posture in terms of joint angles, and, according to (4), (6), and (7), stiffness and viscosity matrices **S** and **V** are

$$\boldsymbol{S} = \boldsymbol{D}\boldsymbol{W}\boldsymbol{S}^{W}\boldsymbol{W}^{-1}, \quad \boldsymbol{V} = \boldsymbol{D}\boldsymbol{W}\boldsymbol{V}^{W}\boldsymbol{W}^{-1}. \tag{15}$$

and $\mathbf{S}^W$ and $\mathbf{V}^W$ are stiffness and viscosity matrices in terms of eigenmovements. If eigenmovements are controlled independently, then these matrices are diagonal with K^S_i and K^V_i as coefficients. As shown in (Alexandrov et al. 2004), in this case matrices **S** and **V** are symmetrical.

The equations (15) can be presented as

$$\mathbf{S}^{-1}\mathbf{DW} = \mathbf{W}(\mathbf{S}^{W})^{-1}, \quad \mathbf{V}^{-1}\mathbf{DW} = \mathbf{W}(\mathbf{V}^{W})^{-1}. \tag{16}$$

If matrices $\mathbf{S}^W$ and $\mathbf{V}^W$ are diagonal then matrices $(\mathbf{S}^W)^{-1}$ and $(\mathbf{V}^W)^{-1}$ are also diagonal, i.e. if eigenmovements are controlled independently then eigenvectors w_i (columns of matrix W) defined by (3) are also the eigenvectors of matrices $\mathbf{S}^{-1}\mathbf{D}$ and $\mathbf{V}^{-1}\mathbf{D}$ with eigenvalues $1/K^S_i$ and $1/K^V_i$ respectively.

3 Results

Fig. 3 shows a representative example of the time course of CG and CP displacements in A-, H-, and K-eigenmovements in response to platform perturbations. The first pulse in platform acceleration caused forward CG displacements in all eigenmovements. The CG displacements, in turn, caused corrective CP displacements in which CG was pushed backward to the initial equilibrium position. Note that the CG and CP displacements in K-eigenmovement nearly coincided due to the low inertia of this eigenmovement.

To evaluate our hypothesis concerning the independent feedback control of eigenmovements, we determined whether the feedback model (13) accurately explains the observed time course of CP displacement in each eigenmovement. To that end, the optimal parameters K^S_i, K^V_i, and τ_i of the regression model (13) were calculated for each eigenmovement. These parameters minimized mean square error E_i between X^{CP}_i calculated by the experimental recordings according to (6) and (8) and that calculated by the regression model (13). The initial CG and CP positions X^{CG}_i and X^{CP}_i in each eigenmovement were referenced to zero. The minimization of E_i is equivalent to the maximization of the coefficient of determination $R^2_i = 1 - E_i/V_i$ where is the variance of X^{CP}_i. For a given delay τ_i, the optimal coefficients K^S_i, K^V_i can be obtained by the standard linear regression procedure. The optimal time delay that provided the maximum of coefficient R^2 was considered as an "effective" delay of the feedback loop for a given eigenmovement, given subject, and given perturbation amplitude. The optimal time delays appeared to be significantly different for different eigenmovements. However, the delays were nearly independent of perturbation amplitudes, and therefore the delay averaged across all perturbation amplitudes was considered as the feedback delay in a given subject for a given eigenmovement. On average across all perturbation amplitudes and subjects, the coefficients of determination R^2 for optimal regression parameters amounted to 0.94±0.05 (SD), 0.96±0.02, and 0.90±0.9 for A-, H-, and K- eigenmovements, respectively. As the coefficient of determination $R^2 \approx 1$, then the regression model holds, and therefore our hypothesis that eigenmovements are independent units of feedback control can be accepted.

Fig. 3 shows typical results from the regression model approximations (13), and Fig. 4, the eigenmovement feedback gains averaged across subjects. Only viscosity in the A-eigenmovement appeared to be significantly dependent on perturbation amplitude. Viscosity slightly decreased as the perturbation amplitude increased.

Because the influence of the perturbation amplitude was insignificant for all feedback gains except one, the individual feedback parameters were averaged across all amplitudes. Table 1 shows parameters of feedback gains for subjects S1–S9 in each eigenmovement.

A multi-variable regression analysis revealed that parameters λ, τ, K^S, and K^V varied across subjects statistically independently for A- and K-eigenmovements, whereas K^S for the H-eigenmovement appeared to be significantly dependent on λ and τ ($p < 0.01$). K^S increased with the increase of λ and the decrease of τ

4 Discussion

4.1 The comparison with the results of the full-state feedback modeling

The full-state linear spring-like feedback model (14) describes the relationship between joint torques and joint angles and angular velocities (Barin 1989;Park et al. 2004). The coefficients of stiffness and viscosity matrices **S** and **V** can be obtained as the optimal parameters of the regression model (14) or by the matrix transformation (15) of coefficients K^S and K^V obtained in the eigenmovement approach. Tables 2 and 3 show the coefficients of these matrices calculated using coefficients K^S and K^V from Table 1 and averaged across all subjects.

The obtained values of stiffness coefficients are in good agreement with the reported data from different experimental paradigms with standing humans (Gurfinkel et al. 1974; Barin 1989; Hof 1998; Winter et al. 1998; Peterka 2002; Park et al. 2004). However, in contrast to our previous study (Park et al. 2004), we did not observe the significant dependence of stiffness on perturbation amplitude. In the present study, we used the perturbation amplitudes not more than 7.5 cm whereas in (Park et al. 2004) the perturbation amplitude reached 15 cm. Therefore, the range of small perturbation amplitudes was not significantly broad enough to expose nonlinear characteristics of feedback control such as gain scaling observed in (Park et al. 2004).

The obtained viscosity coefficients are also inside the range of previous values (Barin 1989; Peterka 2002; Park et al. 2004). Note that the reported range of viscosity coefficients is rather large. For example, V_{11} ranges from $V_{11} \approx$ -90 Nms/rad (Barin 1989) to $V_{11} \approx 400$ Nms/rad (Peterka 2002). As shown in (Alexandrov et al. 2004), the relatively large spread in values for viscosity coefficients could be explained by the difference in the feedback loops delays. When the delay in the regression model is ignored, the viscosity coefficient is underestimateds compared to estimates when the time delay is taken into account. The ignoring of time delay in Barin (1989) and Park et al. (2004) could be the reason that viscosity coefficients estimated in these studies were less than those obtained in the present study (even paradoxically negative [Barin 1989]). In contrast, the longer delay in (Peterka 2002) of about 200 ms might result in the overestimation of the viscosity coefficient V_{11}.

Another source of mismatch in the values of visco-elastic parameters reported here and in Barin (1989) and Park et al. (2004) may relate to the different periods of analysis used in the regression model. In the present study, the trial period included only 1.35 s after the perturbation onset, whereas in Barin (1989) and in Park et al. (2004) it included 6 s and 8 s respectively. Since these periods are comparable with the characteristic time for adjustment of the feedback loop parameters during orthograde posture (Gurfinkel et al. 1995), the feed-forward corrections in the late phase of the response could influence on the estimations of the feedback loop parameters.

In order to compare the accuracy of the eigenmovement and full-state feedback approaches, we calculated the determination coefficients R^2 for the ankle, knee and hip joint torques in both approaches. In the eigenmovement approach, the torques are given by the inversion of equation (6): $\mathbf{T}(t) = \mathbf{U}(t)$ where the components of $\boldsymbol{\eta}$ are given by (12). On average across all subjects and perturbation amplitudes, the eigenmovement approach coefficients R^2 were 0.94±0.05, 0.94±0.04, and 0.92±0.06 for the ankle, knee and hip joint torques respectively. In the full-state feedback approach, the torques are given by equation (14) which is treated as the regression model for the relationship between joint torques and joint angles and angular velocities. On average, across all subjects and perturbation amplitudes, the full-state feedback approach coefficients R^2 were 0.79±0.07, 0.78±0.05 and 0.81±0.06 for the ankle, knee and hip joint torques respectively. Thus, the accuracy of the eigenmovement approach appeared to be higher than that of the full-state feedback approach. Relatively small coefficients R^2 were

obtained for the full-state feedback model in the present study on the basis of the linear regression equation (14). Whereas in (Park et al. 2004), the full-state feedback gains were obtained by minimizing of the error between the experimentally observed kinematics and the results of the direct dynamic solution. This method also provided reasonably good fits (R^2 ~0.92). The similar optimization of direct dynamic solution in the eigenmovement approach resulted in R^2 ~0.95. Therefore, both approaches (eigenmovements and full-state) provided good and comparable fits in the method of optimization of direct dynamic solution. This is reasonable because the eigenmovement approach is a special case of the full-state feedback approach.

On average, across all subjects and perturbation amplitudes, the stiffness coefficients found in the full-state feedback approach amounted to S_{11} = 584 ± 250 Nm/rad, S_{33} = 89 ± 110 Nm/rad, S_{13} = 45 ± 139 Nm/rad, S_{31} = 104 ± 61 Nm/rad, where S_{11} and S_{33} are the ankle and hip joint stiffness coefficients, and S_{13} and S_{31} are the cross-stiffness coefficients. These values are consistent with those obtained in our previous work (Park et al. 2004) and shown in Table 2.

The model of the *joint level* feedback control in which the cross-stiffness and cross-viscosity coefficients are ignored, appeared to be much less accurate than both eigenmovement and full-state feedback control models. In the joint level model, the determination coefficient R^2 amounted to 0.60±0.21, 0.13±0.40 and 0.69±0.23 for the ankle, knee and hip joint torques respectively.

4.2 The advantage of the independent eigenmovement control

Formally, the model of independent eigenmovement feedback control is preferable to both full-state and joint-level models of feedback control because, first, the joint-level model provides poorer accuracy than both eigenmovement and full-state models and, second, the eigenmovement model is less parameterized than the full-state model. The 3-joint full-state model includes 18 free parameters (the 3 x 3 stiffness and 3 x 3 viscosity coefficients), while the model of the independent eigenmovement control requires only 6 parameters (3 stiffness and 3 viscosity coefficients).

However, we believe that its advantage is not only formal. Since the independent eigenmovement control provides such drastic simplification of control in the multijoint biomechanical system, it is reasonable to suggest that the CNS actually uses this advantage. The mentioned simplification relates to the fact that the independent eigenmovement feedback control allows for splitting of the coupled system of dynamic equations into a set of independent equations each one for a separate eigenmovement, and therefore the CNS has the ability to control each eigenmovement independently also in a feed forward manner. The evidence for independent feed forward control of eigenmovements was obtained in our previous study of voluntary upper trunk bending (Alexandrov et al. 2001b), but as shown below, independent feedforward control of eigenmovements is espcially simplified under their independent feedback control. If the suggestion of the independent feedback control holds, then the generation of controlling muscle torques in each eigenmovement for both feedback and feed forward controls is determined by the equation:

$$\eta_i(t) = K_i^S(\xi_i(t-\tau_i) - \xi_i^0(t)) + K_i^V \dot{\xi}_i(t-\tau_i), \quad i = A, H, K, \tag{17}$$

where, according to (4) and (6), kinematic and dynamic eigenmovement amplitudes ξ_i (t) and η_i (t) are generalized coordinates and forces, respectively; ξ_i^0 (t) are the feed forward control signals that determine the change of the equilibrium reference body configuration. Due to the

independent feedback control of each eigenmovement, the dynamic equations (5) for each eigenmovement remain to be independent and take the form

$$\begin{aligned} &-\lambda_i \xi_i(t-\tau_i)+\xi_i \\ &=K_i^S(\xi_i(t-\tau_i)-\xi_i^0(t))K_i^V\xi_i(t-\tau_i). \end{aligned} \tag{18}$$

When ξ_i^0 is fixed, then (18) corresponds to the equation of equilibrium maintenance about equilibrium body configuration $\xi_i^{eq} = K^S_i\,\xi_i^0 / (K^S_i - 1)$. Voluntary movement is initiated by the feed forward change of the control signal $\xi_i^0(t)$ providing the body movement from the initial to the final equilibrium configuration. According to (18), each *i*-th eigenmovement is controlled by its individual feed forward control signal $\xi_i^0(t)$ independently of other eigenmovements.

To clarify the advantages of independent eigenmovement feedback control, let us consider the time organization of the feed forward control signal in the case of full-state feedback control during a simple one-dimensional movement when all joint angles change synchronously. In this case, the time course of joint angles $\Delta\boldsymbol{\phi}(t)=\mathbf{e}\zeta(t)$, where **e** is the unit vector that determines the ratio between ankle, knee and hip joint angles, and $\zeta(t)$ determines the movement time course. As shown by principal component analysis, such movement is actually observed, for example, during human voluntary upper trunk bending (Alexandrov et al. 1998). Then, according to (2) and (14), the dynamic equation takes the following form:

$$\boldsymbol{C}\ddot{\boldsymbol{\varphi}}(t)-\boldsymbol{D}\dot{\boldsymbol{\varphi}}(t)=-\boldsymbol{S}(\boldsymbol{\varphi}(t)-\boldsymbol{\varphi}^0(t))-\boldsymbol{V}\dot{\boldsymbol{\varphi}}(t), \tag{19}$$

where $\boldsymbol{\phi}^0(t)$ is the vector of the feed forward control signal that determines the change of the equilibrium reference body configuration. According to (19), the control signal $\boldsymbol{\phi}^0(t)$ that provides this movement is

$$\Delta\boldsymbol{\varphi}^0(t)=\boldsymbol{e}_0\zeta(t)+\boldsymbol{e}_1\dot{\zeta}(t)+\boldsymbol{e}_2\ddot{\zeta}(t), \tag{20}$$

where $\mathbf{e}_0 = \mathbf{e} - \mathbf{S}^{-1}\,\mathbf{De}$, $\mathbf{e}_1 = \mathbf{S}^{-1}\,\mathbf{Ve}$, $\mathbf{e}_2 = \mathbf{S}^{-1}\,\mathbf{Ce}$. Generally, the vectors $\mathbf{e}_0$, $\mathbf{e}_1$ and $\mathbf{e}_2$ are not collinear and the time courses of $\zeta(t)$, $\dot{\zeta}(t)$ and $\ddot{\zeta}(t)$ are very different so that the trajectory of the control signal $\Delta\boldsymbol{\phi}^0(t)$ in the joint angle space must be rather complex even to provide this simple movement. On the contrast, this signal is simple when, first, the movement direction **e** coincides with one of the eigenvectors $\mathbf{w}_i$ given by (4) and, second, **e** is the eigenvector of matrices $\mathbf{S}^{-1}\mathbf{D}$ and $\mathbf{S}^{-1}\mathbf{V}$. According to (16), in this case, $\mathbf{e}_0=\mathbf{w}_i(1-1/K^S_i)$, $\mathbf{e}_1=\mathbf{w}_iK_i^V/K_i^S$, and $\mathbf{e}_2=\mathbf{w}_i\,\lambda_i/K^S_i$, where K_i^S and K_i^V are the gains of the feedback loop for *i*-th eigenmovement. Hence, under these conditions, the control signal $\Delta\boldsymbol{\phi}^0(t)$ in (20) is one-dimensional in the joint angle space and directed along the vector $\mathbf{e}=\mathbf{w}_i$. It should be emphasized that two of the above conditions for **e** are equivalent to the suggestion that eigenmovements of the dynamic equations (2) are under independent feedback control. Note, that the one-dimensional movement $\Delta\boldsymbol{\phi}(t)$, observed during the human upper trunk bending, is actually directed close to the hip eigenvector $\mathbf{w}_H$ (Alexandrov et al. 1998,2001b).

We consider that the A- and H- eigenmovements constitute the biomechanical basis for “ankle” and “hip” strategies described by Horak and Nashner (1986). First in the A-eigenmovement, as in the ankle strategy, the ankle joint dominates. In the H-eigenmovement, the approximate ratio between hip and ankle motions is −4:1 (Alexandrov et al. 2001b) which is close to the ratio of hip and ankle motions in the hip strategy (Kuo and Zajac 1993). Second, the high inertial A- eigenmovement is efficient in restoring the center of gravity (CG) position destabilized by slow perturbations whereas the five times less inertial H- eigenmovement is efficient in restoring the CG position for fast perturbations. It was experimentally demonstrated that, the ankle strategy is used in response to slow perturbations, whereas, the relative

contribution of hip strategy gradually increases with the increase in perturbation velocity (Runge et al. 1999). The dominance of either hip or ankle eigenmovement under the fast or slow perturbation conditions was explained in (Alexandrov et al. 2004). The observations of the independent use of the hip and ankle strategies under different experimental conditions (Nashner and McCollum 1985; Horak and Nashner 1986) are also in favor with the suggestion that eigenmovements could be independently controlled by CNS as the entire motion units.

4.3 Stability of posture maintenance

The majority of previous studies on equilibrium stability of upright standing were based on the simple biomechanical model of the human body as one-dimensional inverted pendulum (Morasso and Schieppati 1999; Winter et al. 2001; Kiemel et al. 2002; Peterka 2002; Micheau et al. 2003). The previous studies that took into account multijoint properties of the body (Barin 1989; Park et al. 2004), did not take into account the delays in the feedback loop. However, the existence of delays essentially complicates postural stabilization and requires the strict adjustment of the feedback loop gains to time delays (Matthews 1972; Rack 1981). In the present study, we take into account both the feedback loop delays and multijoint body configuration. In the frame of our hypothesis that eigenmovements are independent units of feedback control during upright standing, we analyzed equilibrium stability independently for each eigenmovement. Using feedback parameters (gains and delays) taken from the Results section, a closed-loop equation is obtained by inserting (12) into (5):

$$\begin{aligned} &-\lambda_i \ddot{\xi}_i(t) + \xi_i(t) - K_i^S \xi_i(t-\tau_i) - K_i^V \dot{\xi}_i(t-\tau_i) \\ &= -\chi_i a_x(t) - K_i^S \xi_{0i}. \end{aligned} \tag{21}$$

The eigenvalues μ of (21) satisfy the equation:

$$\mu^2 \lambda_i - 1 + K_i^S e^{-\mu\tau_i} + \mu K_i^V e^{-\mu\tau_i} = 0 \tag{22}$$

Equation (22) has an infinite number of roots (see Appendix C). The solution of (21) is stable only if the real parts of all eigenvalues μ are non-positive ($\mathrm{Re}(\mu) \leq 0$). As shown in Appendix C, this is valid for $|\mu\tau_i| >> 1$. If $|\mu\tau_i| \sim 1$, then the roots of (22) can be easily found by numerical solution of the system of equations (C1). Table 4 shows all of the roots μ of (22) with $\mathrm{Re}(\mu) < -20$ calculated numerically for each subject and for each eigenmovement using the parameters λ, K^S, K^V, and τ, which are represented in Table 1. Because the roots of (22) are conjugate, only the roots with positive imaginary parts are shown in Table 4. The roots with $\mathrm{Re}(\mu) < -20$ that are not presented in Table 2 correspond to the movements that are quickly damped.

As shown in Table 4, all of the roots of (22) have the non-positive real parts, except for subject S2's K-eigenmovement. Thus, the calculated spring-like feedback parameters provided stability for upright stance in all subjects except subject S2. However, subject S2 also demonstrated stable equilibrium despite the positive sign of the real part of one of roots in (22), calculated by subject S2's individual feedback loop parameters. The erroneous prediction that this subject would not be able to maintain stable posture using only feedback control could be explained by the relatively low accuracy in estimating the feedback parameter K^V in the K-eigenmovement (see the high SD for K^V in the K-eigenmovement in Table 1 and Fig. 4).

For the maintenance of stable stance, the values of parameters K^S and K^V must be inside the limited stability region, defined as a region in which all roots of (22) have non-positive real parts. Fig. 5 shows the borders of stability regions for A-and H- eigenmovements obtained by the numerical solution of (C1) for subjects with the largest (S4, S5; thin lines) and the smallest (S7, S8; thick lines) values of feedback time delays (Table 1, bold underscored). The stability

regions appeared to be restricted by the upper and lower limits for both parameters K^S and K^V. The lower limit for K^S was equal to 1: the condition $K^S \geq 1$ was evidently required to compensate for the *negative stiffness* of gravity forces in the inverted pendulum (see (16)). The stability region increased when τ decreased. The values of K^S and K^V are shown by the open (largest delays; S7, S8) and closed (smallest delays; S4, S5) circles. Note that all circles are located inside the corresponding individual stability regions. However, the closed circles, being inside their corresponding stability regions for small delays, are outside the stability regions for large delays, illustrating the necessity of adjusting the feedback gains to individual time delays for the maintenance of stable upright stance.

As shown in Fig. 5, stability regions in the H-eigenmovement were much smaller than those in the A-eigenmovement, even though there were larger delays in the A-eigenmovement compared those in the H-eigenmovement. The difference in the sizes of stability regions in the eigenmovements resulted from the large difference in eigenmovement inertia: $\lambda_A >> \lambda_H$. Thus, the size of the stability region increases as the delay in the feedback loop decreases and as the eigenmovement inertia increases.

Because the border of the stability region is completely determined by eigenmovement inertia λ and time delay τ (see (22)), a dependence of gain coefficients on these parameters could be expected. However, the statistically significant dependence of gain coefficients on these parameters was not observed in the A-eigenmovement. In contrast, the statistically significant dependence of K^S on λ and τ was observed for the H-eigenmovement: K^S decreased with the decrease of λ and the increase of τ. This shift of K^S followed the shift of the right border of the stability region when λ and τ changed, as shown in Fig. 5. Thus, across subjects, as the right border of the stability region moved to the left, the point on the plane (K^S, K^V) also moved to the left, preserving its location inside the individual stability regions for all subjects.

Thus, the present study shows that in spite of the delays in the feedback control, this control provides the stability of the equilibrium maintenance for the human body as a multi-joint biomechanical system. Note that the existence of delays makes the requirements for the individual adjustment of the feedback gains more severe. In this case they are limited both from up and below (see Fig. 5). On the contrast, in the case without delay (Winter et al. 1998,2001;Morasso and Schieppati 1999), these gains are usually restricted only from below.

4.4 Mechanisms of feedback control

Like Peterka (2002), we consider that the obtained time delays and gain parameters of the feedback loop represent some averaged values resulting from both “passive” (without delay) and “active” (with different time delays) mechanisms. As shown in Alexandrov et al. (2004), the “passive” mechanisms are responsible for the ankle torque production during the first 80 ms after perturbation onset. While thereafter, the “active” mechanisms dominate. These mechanisms cannot be limited to the short latency (40–60 ms) stretch-reflex loop. Specifically, a significant cross-coupling interaction between hip and ankle joints (Park et al. 2004) cannot be explained by the stretch-reflex loop because these joints have no common multi-articular muscles, and the stretch-reflex cross-coupling is weak compared to the feedback on the muscle itself (He et al. 1991; Smeets and van der Gon 1993). Therefore, long-latency, central feedback loops are involved in combination with feedback loops without delay and with short delays. The systems that can contribute to the long-latency feedback for posture control are visual, vestibular, proprioceptive, and tactile (Horak and Macpherson 1996).

With each eigenmovement under independent feedback control, the control system must be capable of estimating the contribution of each eigenmovement into the current body configuration. As the proprioceptive system supplies the CNS with information about the

current body configuration, the proprioceptive system may be the most important for postural stabilization during upright standing (Horak and Macpherson 1996).

In principle, it is possible to modify the feedback model (12) by representing joint torques as a superposition of torques generated by passive and active feedback mechanisms. However, as shown by Peterka (2002), due to the dominant role of active mechanisms, the ignorance of the passive mechanisms does not significantly decrease the accuracy of the feedback model. Thus, the value of the stiffness obtained with the active single-loop model is close to the sum of those in the double-loop model whereas the delay in the single-loop model appears to be slightly smaller than in the active loop in the double-loop model. We decided, therefore, not to complicate the model (12) being aware that it reflects the superposition of several feedback mechanisms with and without different delays and that the obtained “effective” delay is the weighted average of delays in several loops.

The obtained time delay in the feedback loop of the largest inertial A-eigenmovement was about 120 ms, of the middle-inertia H-eigenmovement - 66 ms, and of the least inertia K-eigenmovement - 12 ms (Table 1). This result might reflect the dominance of the longest latency loops in the control of A-eigenmovement, the dominance of the middle-latency loops in the control of H-eigenmovement, and the dominance of the passive mechanism in the control of K-eigenmovement. Note that the values of the first two delays are consistent with reported latencies of ankle- and hip-muscle EMG responses to posture perturbations (Horak and Nashner 1986;Diener et al. 1988;Horak et al. 1989). Note also that the delay in the control of H-eigenmovement is close to the delay in the spinal loop: about 35 ms is the delay in the stretch-reflex loop itself (Koshland and Hasan, 2000) and about 25 ms is the delay of transformation of muscle activation into the muscle torque (Hainaut et al. 1981;Zhao and Wu 1996). Thus, at least three mechanisms (“passive”, spinal and supraspinal) contribute to the feedback control of equilibrium maintenance.

In our study, feedback control was almost linear. As shown in Fig. 4, feedback gains demonstrated only weak dependence on the perturbation amplitude. The slight decrease of the stiffness and viscosity coefficients in A-eigenmovement, with the corresponding increase of the perturbation amplitude, is consistent with the results from Peterka (2002) and Park et al. (2004), who reported similar saturation behavior of the feedback gain at the ankle joint. Park et al. (2004) hypothesized that this saturation reflects biomechanical constraints limiting the amount of available ankle torque. Peterka (2002) suggested that the change in the feedback gains reflects a change in the relative contribution of different sensory systems to the feedback control. The sensory selection mechanism might be dependent on the perturbation amplitude. However, in the present study, the non-linear effects of saturation in the feedback loops were smaller than those in (Park et al. 2004) because we restricted the analysis by the data with twice smaller perturbation amplitudes.

Many questions still remain unanswered, such as: How does the CNS integrate signals from different sensory modalities to estimate the contribution of each eigenmovement to the current body configuration? How are corrective forces generated in response to deviations in each eigenmovement from an equilibrium position? Answers to these questions might be found in the framework of modern theories concerning the internal representation of the human body. The internal representation of eigenmovement biomechanical characteristics and the corresponding feedback loop parameters might be stored in the cerebellum (Wolpert et al. 1998).

Acknowledgements

The study was supported by RFBR 04-01-00215-a, 04-04-48989-a, 02-04-48410a, 01-04-48924a, RFH 00-06-00248a, NIH-AG06457. The authors thank Dr. S. Oster for careful reading of the manuscript and useful remarks.

References

Alexandrov AV, Frolov AA, Massion J. Axial synergies during human upper trunk bending. Exp Brain Res 1998;118:210–220. [PubMed: 9547090]

Alexandrov AV, Frolov AA, Massion J. Biomechanical analysis of movement strategies in human forward trunk bending. I. Modeling. Biol Cybern 2001a;84:425–434. [PubMed: 11417054]

Alexandrov AV, Frolov AA, Massion J. Biomechanical analysis of movement strategies in human forward trunk bending. II. Experimental study. Biol Cybern 2001b;84:435–443. [PubMed: 11417055]

Alexandrov AV, Frolov AA, Horak FB, Carlson-Kuhta P, Park S. Biomechanical analysis of strategies of equilibrium control during human upright standing. Russian J Biomech 2004;8(3):28–42.

Barin K. Evaluation of a generalized model of human postural dynamics and control in the sagittal plane. Biol Cybern 1989;61:37–50. [PubMed: 2742913]

Corless RM, Gonnet GH, Hare DEG, Jeffrey DJ, Knuth DE. On The Lambert W Function. Advances in Computational Mathematics 1996;5:329–359.

Diener H, Horak F, Nashner LM. Influence of stimulus parameters on human postural responses. J Neurophysiol 1988;59:1888–1895. [PubMed: 3404210]

Feldman AG, Ostry DJ. A critical evaluation of the force control hypothesis in motor control. Exp Brain Res 2003;153(3):275–88. [PubMed: 14610628]

Fitzpatrick R, Burke D, Gandevia SC. Loop gain of reflexes controlling human standing measured with the use of postural and vestibular disturbances. J Neurophysiol 1996;76:3994–4008. [PubMed: 8985895]

Gurfinkel VS, Lipshits MI, Popov K Ye. Is the stretch reflex the main mechanism in the system of regulation of the vertical posture of man? Biofizika 1974;19:744–748. [PubMed: 4425696]

Gurfinkel VS, Ivanenko YuP, Levik YuS, Babakova IA. Kinesthetic reference for human orthograde posture. Neuroscience 1995;68:229–243. [PubMed: 7477928]

Hainaut K, Duchateau J, Desmedt J. Differential effects on slow and fast motor units of different programs of brief daily muscle training in man. In: Desmedt J (ed) Motor units types, recruitment and plasticity in health and disease. Basel: Karger 1981;9:241–249.

He J, Levin VS, Loeb GE. Feedback gain for correcting small perturbations to standing posture. IEEE Trans Autom Control 1991;36:322–332.

Hof AL. In vivo measurement of series elasticity release curve of human triceps surae muscle. J Biomech 1998;31:793–800. [PubMed: 9802779]

Horak FB, Macpherson JM (1996) Postural orientation and equilibrium. In: L.B. Rowell & J.T. Shepherd (eds) Handbook of Physiology. Section 12.. Oxford University Press. New York-Oxford, pp 255–292

Horak FB, Nashner LM. Central programming of postural movements: adaptation to altered support surface configurations. J Neu-rophysiol 1986;55:1369–1381.

Horak F, Diener H, Nashner L. Influence of central set on human postural responses. J Neurophysiol 1989;62:841–853. [PubMed: 2809706]

Kiemel T, Kelvin SO, Jeka JJ. Multisensory fusion and stochastic structure of postural sway. Biol Cybern 2002;87:262–277. [PubMed: 12386742]

Koshland GF, Hasan Z. Electromyographic responses to a mechanical perturbation applied during impending arm movements in different directions: one-joint and two-joint conditions. Exp Brain Res 2000;132(4):485–499. [PubMed: 10912829]

Kuo A, Zajac F. Human standing posture: Multijoint movement strategies based on biomechanical constraints. Prog Brain Res 1993;97:349–358. [PubMed: 8234760]

Kuo AF. An optimal control model for analyzing human postural balance. IEEE TransBiomed Engin 1995;42:87–101.

Matthews PBC (1972) Mammalian muscle receptors and their central actions. London: Arnold

Morasso PG, Schieppati M. Can muscle stiffness alone stabilize upright standing? J Neurophysiol 1999;83:1622–1626. [PubMed: 10482776]

Micheau P, Kron A, Bourassa P. Evaluation of the lambda model for human postural control during ankle strategy. Biol Cy-bern 2003;89:227–236.

Nashner LM, McCollum G. The organization of human postural movements: a formal basis è experimental synthesis. Behav Brain Sci 1985;8:135–172.

Orfandis SJ (1996) Introduction to signal processing. Prentice-Hall, Englewood Cliffs, NJ

Park S, Horak FB, Kuo AD. Postural feedback responses scale with biomechanical constraints in human standing. Exp Brain Res 2004;154:417–427. [PubMed: 14618285]

Peterka RJ. Sensorimotor integration in human postural control. J Neurophysiol 2002;85:1097–1118. [PubMed: 12205132]

Rack PMH (1981) Limitation of sensory feedback in control of posture and movement. In: The nervous system. Motor control. Bethesda, MD: Am. Physiol. Soc. section. 1, vol. II: 229–256

Runge CF, Shupert CL, Horak FB, Zajac FE. Ankle hip postural strategies defined by joint torques. Gait Posture 1999;10:161–170. [PubMed: 10502650]

Smeets JBJ, van der Gon JJD. An unsupervised neural network model for the development of reflex co-ordination. Biol Cybern 1993;70:417–425. [PubMed: 8186302]

van der Kooij H, Jacobs R, Koopman B, Grootenboer H. A mul-tisensory integration model of human stance control. Biol Cybern 1999;80:299–308. [PubMed: 10365423]

van der Kooij H, Jacobs R, Koopman B, van der Helm F. An adaptive model of sensory integration in a dynamic environment applied to human stance control. Biol Cybern 2001;84:103–115. [PubMed: 11205347]

Winter DA (1990). Biomechanics and motor control in human movement (Second ed.). New York: John Wiley and Sons

Winter DA, Patla AE, Prince F, Ishac M, Gielo-Perczak K. Stiffness control of balance in quiet standing. J Neurophysiol 1998;80:1211–1221. [PubMed: 9744933]

Winter DA, Patla AE, Rietdyk S, Ishac M. Ankle muscle stiffness in the control of balance during quiet standing. J Neurophysiol 2001;85:2630–2633. [PubMed: 11387407]

Wolpert DM, Miall RC, Kawato M. Internal models in the cerebellum. TrendsCogn Sci 1998;2:338–347.

Yang JF, Winter DA, Wells RP. Postural dynamics in the standing human. Biol Cybern 1990;62:309–320. [PubMed: 2310785]

Zhao W, Wu P (1996) Effect of time-delay in feedback on human stability – a computer study. 20th annual meeting of the American Society of Biomechanics, Atlanta

APPENDIX A. Motion equation

The motion equation has a simple form in terms of segment angles θ_i with respect to the vertical:

$$\boldsymbol{C}'(\boldsymbol{\theta})\ddot{\boldsymbol{\theta}} - \boldsymbol{D}'(\boldsymbol{\theta}) + \boldsymbol{A}'(\dot{\boldsymbol{\theta}}, \boldsymbol{\theta}) = \boldsymbol{NT} + \boldsymbol{P}'_{a_X}, \tag{23}$$

where **T** is the vector of joint torques; matrix **N** is

$$\boldsymbol{N} = \begin{pmatrix} 1 & -1 & 0 \\ 0 & 1 & -1 \\ 0 & 0 & 1 \end{pmatrix};$$

and the elements of the inertial matrix $\mathbf{C}'(\theta)$, the gravitational matrix $\mathbf{D}'(\theta)$, the components of the vector of centripetal and Coriolis forces $\mathbf{A}'(\theta, d\theta/dt)$, and the components of the perturbation vector $\mathbf{P}'$ are

$$C'_{UU} = m_U c_U^2 + I_U;$$

$$C'_{UM} = C'_{MU} = m_U c_U l_M \cos(\theta_U - \theta_M);$$

$$C'_{UL} = C'_{LU} = m_U c_U l_L \cos(\theta_U - \theta_L);$$

$$C'_{MM} = m_M c_M^2 + m_U l_M^2 + I_M;$$

$$C'_{ML} = C'_{LM} = (m_M c_M l_L + m_U l_L l_M) \cos(\theta_M - \theta_L);$$

$$C'_{LL} = m_L c_L^2 + (m_M + m_U) l_L^2 + I_L;$$

$$D'_{UU} = Z_U g \sin(\theta_U) \Big/ \theta_U;$$

$$D'_{MM} = Z_M g \sin(\theta_M) \Big/ \theta_M;$$

$$D'_{LL} = Z_L g \sin(\theta_L) \Big/ \theta_L;$$

$$D'_{UM} = D'_{UL} = D'_{MU} = D'_{UM} = D'_{LU} = D'_{LM} = 0;$$

$$P'_i = Z_i \cos(\theta_i);$$

$$Z_L = m_L c_L + (m_M + m_U) l_L;$$

$$Z_M = m_M c_M + m_U l_M;$$

$$Z_U = m_U c_U;$$

$$A'_U = m_U c_U (l_L \sin(\theta_U - \theta_L)\theta_L^2 + l_M \sin(\theta_U - \theta_M)\theta_M^2);$$

$$A'_M = (m_M c_M l_L + m_U l_L l_M) \sin(\theta_M - \theta_L)\theta_L^2 - m_U c_U l_M) \sin(\theta_U - \theta_M)\theta_u^2;$$

$$A'_L = -(m_M c_M l_L + m_U l_L l_M) \sin(\theta_M - \theta_L)\theta_M^2 - m_U c_U l_L \sin(\theta_U - \theta_L)\theta_u^2.$$

where the parameters *m*, *I*, *l*, and *c* for each of the three body segments are, respectively, its mass, moment of inertia about the center of mass, and the length and distance of the segment center of mass from its distal end. Subscript *i* applied to the body segment indicates the lower (*i* = *L*, shanks), middle (*i* = *M*, thighs), and upper (*i* = *U*, trunk with arms and head) segments.

Motion equation (1) is written in terms of joint angles ϕ and can be easily obtained from equation (A1) by changing the variables $\boldsymbol{\theta} = \mathbf{R}\boldsymbol{\phi}$, where $R = (N^{-1})^T$. Then $C(\phi) = \boldsymbol{R}^T C'(\theta)\boldsymbol{R}$, $\boldsymbol{D}(\phi) = \boldsymbol{R}^T \boldsymbol{D}'(\theta)\boldsymbol{R}$, $\boldsymbol{A}(\phi, \dot{\phi}) = \boldsymbol{R}^T \boldsymbol{A}'(\theta, \dot{\theta})$ and $P = \mathbf{R}^T\mathbf{P}'$.

In the linear approximation about the erect body position, (1) takes the form of (2), where $\mathbf{C} = \mathbf{C}(\mathbf{0})$, $\mathbf{D} = \mathbf{D}(\mathbf{0})$, $\mathbf{P} = \mathbf{P}(\mathbf{0})$, and $\mathbf{A} = \mathbf{0}$.

APPENDIX B. Relationship between center of gravity and center of pressure in individual eigenmovements

The antero-posterior center of gravity (CG) position is given by

$$X^{CG} = -\frac{((m_L c_L + m_M l_M + m_U l_U)\sin(\phi_A) + (m_M c_M + m_U l_U)\sin(\phi_A + \phi_K) + m_U c_U \sin(\phi_A + \phi_K + \phi_H))}{M} \quad (24)$$

where M is the whole body mass. The subscripts A, K, and H indicate ankle, knee, and hip joints. Positive X^{CG} corresponds to the forward CG displacement.

The center of pressure (CP) position in the antero-posterior direction X^{CP} is:

$$X^{\mathrm{CP}} = \frac{T_A}{F_Y} \tag{25}$$

where T_A is the torque at the ankle joint and $F_Y = M(g + \ddot{Y}^{CG})$ is the vertical reaction force.

According to (24) written in the linear approximation $X^{CG} = \mathbf{B}^{\mathrm{T}} \boldsymbol{\phi}$ where $\mathbf{B}^{\mathrm{T}} = -\mathbf{D}_{\mathrm{A}}{}^{\mathrm{T}}/Mg$ and $\mathbf{D}_{\mathrm{A}}{}^{\mathrm{T}}$ is the first row of gravitational matrix $\mathbf{D}$ (see Appendix A), so that the elements of row $\mathbf{B}^{\mathrm{T}}$ are:

$$B_A = -\frac{(m_L c_L + m_M l_M + m_U l_U + m_M c_M + m_U l_U + m_U c_U)}{M};$$

$$B_K = -\frac{(m_M c_M + m_U l_U + m_U c_U)}{M};$$

$$B_H = -\frac{m_U c_U}{M}.$$

According to equation (4), in the i-th eigenmovement, $\boldsymbol{\phi} = \mathbf{w}_i \xi_i$. Consequently, the CG position in the i-th eigenmovement is $X_i^{\mathrm{CG}} = \mathbf{B}^{\mathrm{T}} \mathbf{w}_i \xi_i$, which corresponds to (8), where $b_i = \mathbf{B}^{\mathrm{T}} \mathbf{w}_i$ (i = A, K, H).

Equation (25) in the linear approximation takes the form $X^{\mathrm{CP}} = T_A/Mg$. According to (6) and (7), in the i-th eigenmovement, $T_{Ai} = u_{Ai}\eta_i$, where $u_{Ai} = -\mathbf{D}_{\mathrm{A}}{}^{\mathrm{T}} \mathbf{w}_i = \mathbf{B}^{\mathrm{T}} \mathbf{w}_i \, Mg = Mgb_i$. Consequently, $X_i^{\mathrm{CP}} = b_i \eta_i$ (cf. (8) and (5)) is directly transformed into (9).

APPENDIX C. Roots of equation (22)

Equation (22) for complex $\mu = a_1 + b_1 i$ can be rewritten in the form of the system of two real equations:

$$\mathrm{Re}\,(F_1(a_1, b_1)) = \mathrm{Im}\,(F_1(a_1, b_1)) = 0, \tag{26}$$

where $F_1(a_1, b_1) = (a_1 + b_1 i)^2 \lambda - 1 + K^S e^{-ta_1\tau} [\cos(b_1\tau) + i \sin(b_1\tau)] + (a_1 + b_1 i) K^V e^{-ta_1\tau} [\cos(b_1\tau) + i \sin(b_1\tau)]$.

For $|\mu| >> 1$, the roots of (22) can be found from the equation

$$z \exp(z) = -q, \tag{27}$$

where $z = \mu\tau$ and $q = K^V \tau / \lambda^g$ The equation (27) defines function z on q which is called the function of Lambert and which is known to have infinite number of values for each given q (Corless et al. 1996), i.e. (27) has the infinite number of roots. Similarly to (26), the equation (27) can be presented as a system of real equations:

$$\mathrm{Re}\,(z \exp(z)) = -q, \quad \mathrm{Im}\,(z \exp(z)) = 0. \tag{28}$$

In the explicit form, the system (28) looks like:

$$e^{a_2}(a_2 \cos b_2 - b_2 \sin b_2) = -q, \quad b_2 \cos b_2 + a_2 \sin b_2 = 0.$$

where $a_2 = \mathrm{Re}(z)$ and $b_2 = \mathrm{Im}(z)$.

The substitution of a_2 from the second equation into the first one gives:

$$\left(\frac{b_2}{\sin b_2}\right) \exp\left(\frac{-b_2 \cos b_2}{\sin b_2}\right) = q.$$

If $b_2 >> 1$ then $b_2 = 2\pi n + \pi/2\text{-}\varepsilon$, where n is a large natural number and $\varepsilon \approx \ln(2\pi n/q)/(2\pi n) << 1$. Consequently, $a_2 \approx -\ln(2\pi n/q)$. Thus, for $|\mu\,\tau| >> 1$, all roots $\mu = z/\tau$ of (22) have negative real parts $\mathrm{Re}(\mu)=a_2/\tau$.

The border of stability region in coordinates K^S and K^V can be easily obtained numerically from the system of equations (26) regarded as the system of equations relative to K^S and K^V in dependence on b_1 for a_1=0. This border separates the stability region where $a_1 < 0$ and the instability region where $a_1 > 0$.

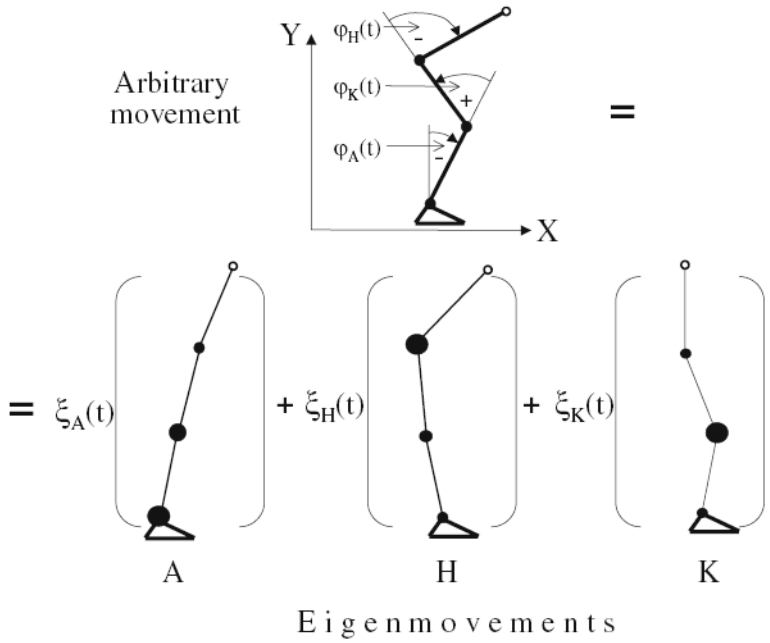

Fig. 1.

Representation of the arbitrary movement of the human body in the sagittal plane, as a superimposition of eigenmovements. The stick diagrams and the size of circles illustrate the relative contributions of each joint to eigenmovement kinematics (joint angles) and dynamics (joint torque). The ankle joint dominates in the A-eigenmovement, the hip joint – in the H-eigenmovement, and the knee joint – in the K-eigenmovement

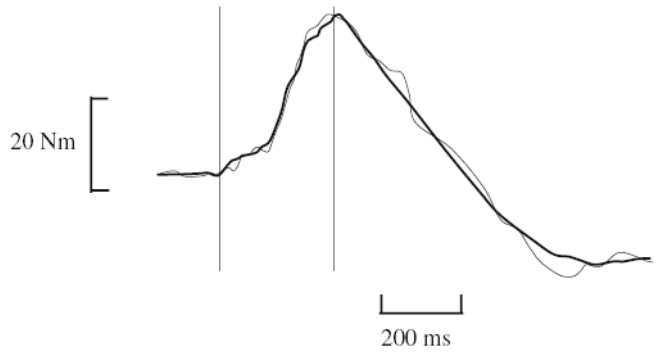

Fig. 2.

Ankle joint torque calculated by the kinematic data (thick line) according to equation (2) and directly measured by the force platform (thin line). Representative data averaged across all trials of subject S1 with a perturbation amplitude of 3.0 cm. Vertical bars indicate the onset and offset of platform movement

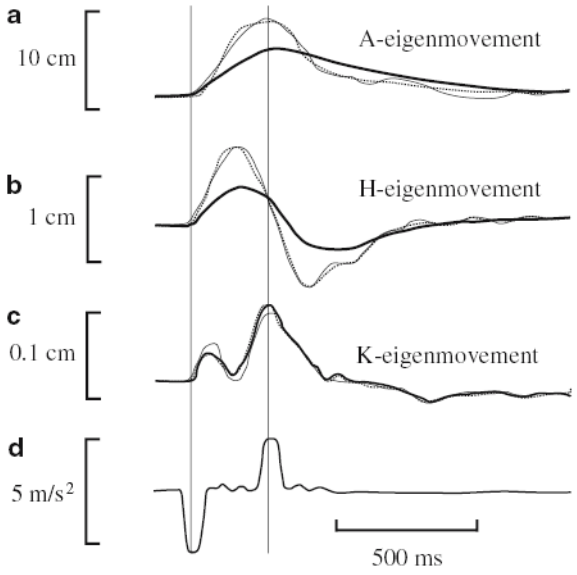

Fig. 3.

Center-of-gravity (thick solid lines) and center-of-pressure (thin solid lines) displacements relative to the moving platform in three eigenmovements (a, b, c) and platform acceleration (d). Representative data averaged across all trials of subject S1 with a perturbation amplitude of 7.5 cm. Vertical bars indicate the onset and offset of platform movement. A dotted line corresponds to the center of pressure regression model fit. Note the different scales for the ordinate axes in a, b, and c. (Modified from Alexandrov et al., 2004)

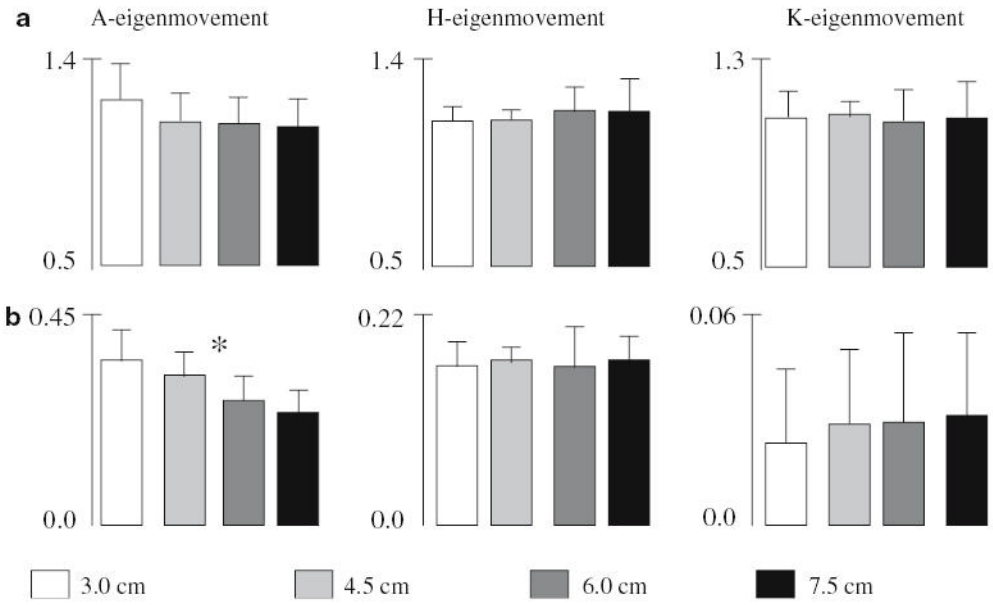

Fig. 4.

The eigenmovement-feedback gains (a) K^S and (b) K^V averaged across subjects for different perturbation amplitudes. Only K^V in A-eigenmovement significantly depends on the perturbation amplitude (marked by asterisk)

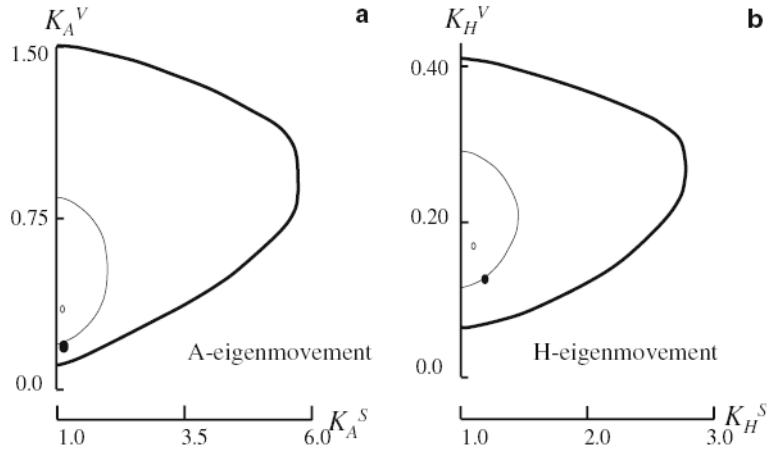

Fig. 5.

Borders of stability regions in coordinates K^S and K^V for (a) A- and (b) H- eigenmovements in subjects with the largest feedback time delays (thin lines) and in subjects with the smallest time delays (thick lines) from Table 1 (bold underscored, S5 and S7 for A-eigenmovement, S4 and S8 for H-eigenmovement). Open and closed circles indicate the experimentally obtained values K^S and K^V for subjects with the largest (S5 and S4) and the smallest (S7 and S8) time delays, respectively. Note the different scales for the axes in (a) and (b)

Table 1

Ankle (A), hip (H) and knee (K) eigenmovements characteristics of subjects S1–S9 averaged across perturbation amplitudes*. Bold underscoring represents characteristics of subjects with the largest and the smallest time delays in A- and H- eigenmovements

	A-eigenmovement			
S	**λ $10^{-2}s^2$**	**τ ms**	**K^S**	**K^V s**
1	10.65	93.7 ± 12.5	1.16 ± 0.14	0.30 ± 0.07
2	10.20	118.8 ± 8.0	1.09 ± 0.08	0.30 ± 0.02
3	9.79	110.4 ± 8.1	1.18 ± 0.16	0.34 ± 0.06
4	9.80	108.3 ± 6.8	1.19 ± 0.15	0.36 ± 0.07
5	9.85	**150.3** ± 5.0	1.09 ± 0.06	0.37 ± 0.06
6	9.88	133.3 ± 29.1	1.20 ± 0.19	0.33 ± 0.09
7	9.49	**83.3** ± 19.1	1.12 ± 0.15	0.21 ± 0.09
8	9.54	139.1 ± 31.1	1.05 ± 0.05	0.26 ± 0.06
9	10.75	150.0 ± 8.4	1.24 ± 0.07	0.34 ± 0.05
Av*	**10.00 ± 0.42**	**120.8 ± 22.7**	**1.15 ± 0.06**	**0.31 ± 0.05**
	H-eigenmovement			
S	λ $10^{-2}s^2$	τ ms	K^S	K^V s
1	1.68	56.3 ± 12.5	1.31 ± 0.16	0.17 ± 0.01
2	1.53	56.7 ± 4.1	1.23 ± 0.02	0.16 ± 0.01
3	1.56	68.6 ± 4.2	1.10 ± 0.06	0.22 ± 0.02
4	1.49	**75.0** ± 4.0	1.08 ± 0.02	0.17 ± 0.02
5	1.53	72.1 ± 8.0	1.13 ± 0.03	0.16 ± 0.01
6	1.55	66.7 ± 6.7	1.11 ± 0.05	0.19 ± 0.02
7	1.39	64.6 ± 4.1	1.10 ± 0.05	0.16 ± 0.01
8	1.51	**50.0** ± 11.7	1.19 ± 0.10	0.13 ± 0.01
9	1.64	85.4 ± 4.3	1.10 ± 0.03	0.17 ± 0.02
Av*	**001.54 ± 0.08**	**066.1 ± 10.20**	**001.15 ± 0.07**	**000.17 ± 0.02**
	K-eigenmovement			
S	λ $10^{-2}s^2$	τ ms	K^S	K^V s
1	0.189	8.3 ± 7.3	1.01 ± 0.01	0.012 ± 0.009
2	0.191	8.3 ± 8.0	1.27 ± 0.10	0.006 ± 0.004
3	0.172	14.0 ± 4.4	1.04 ± 0.04	0.04 ± 0.005
4	0.180	17.0 ± 13.0	1.01 ± 0.01	0.03 ± 0.005
5	0.176	12.5 ± 8.3	1.01 ± 0.01	0.04 ± 0.02
6	0.174	13.0 ± 10.1	1.15 ± 0.14	0.04 ± 0.03
7	0.178	8.5 ± 8.0	1.02 ± 0.01	0.05 ± 0.02
8	0.168	13.1 ± 7.5	1.16 ± 0.18	0.05 ± 0.02
9	0.197	16.6 ± 11.7	1.03 ± 0.01	0.03 ± 0.014
Av*	**0.18 ± 0.09**	**12.3 ± 3.2**	**1.08 ± 0.08**	**0.033 ± 0.015**

Table 2

Stiffness coefficients

Study	Stiffness, Nm/rad								
	S_{11}	S_{12}	S_{13}	S_{21}	S_{22}	S_{23}	S_{31}	S_{32}	S_{33}
Present study	602±119	343±67	127±29	343±67	337±54	129±26	127±29	129±26	128±25
Barin 1989	1087	−37	−250	663	171	−72	225	12	119
Park et al. 2004	690÷850	—	170÷270	—	—	—	160÷180	—	160÷220
Gurfinkel et al. 1974	730÷955	—	—	—	—	—	—	—	—
Winter et al. 1998	802±304	—	—	—	—	—	—	—	—
Hof 1998	500÷800	—	—	—	—	—	—	—	—
Peterka 2002	1000÷1500	—	—	—	—	—	—	—	—

Table 3

Viscosity coefficients

Study	Viscosity, Nms/rad								
	V_{11}	V_{12}	V_{13}	V_{21}	V_{22}	V_{23}	V_{31}	V_{32}	V_{33}
Present study	162±42	97±26	38±11	97±26	67±17	33±8	38±11	33±8	24±5
Barin 1989	−93	−147	−46	−63	−95	−29	−28	−37	−10
Park et al. 2004	60÷90	—	40÷90	—	—	—	0÷7	—	15÷30
Winter et al. 1998	346±101	—	—	—	—	—	—	—	—
Peterka 2002	400	—	—	—	—	—	—	—	—

Table 4

The roots μ_i of equation (22) with Re(μ)> −20 and non-negative imaginary parts Im(μ) = 0 calculated for subjects S1-S9 for ankle (A), hip (H), and knee (K) eigenmovements. Bold underscoring represents μ with a positive real part.

	A-eigenmovement				H-eigenmovement				K-eigenmovement			
	$\mu_1(s^{-1})$		$\mu_2(s^{-1})$		$\mu_1(s^{-1})$		$\mu_2(s^{-1})$		$\mu_1(s^{-1})$		$\mu_2(s^{-1})$	
S	Re(μ_1)	Im(μ_1)	Re(μ_2)	Im(μ_2)	Re(μ_1)	Im(μ_1)	Re(μ_2)	Im(μ_2)	Re(μ_1)	Im(μ_1)	Re(μ_2)	Im(μ_2)
1	−1.2	0.7	—	—	−7.1	0	−10.3	1.9	−0.4	2.3	—	—
2	−0.8	0	−1.6	0	−3.6	0	−11.5	6.4	**+1.2**	11.8	—	—
3	−1.7	0.4	−15.4	0	−0.7	0	−5.5	15.2	−1.7	0	−19.8	0
4	−1.25	0	−2.6	0	−0.9	0	−6.3	10.8	−0.8	0	−8.5	0
5	−0.5	0	−4.3	2.5	−1.8	0	−7.0	9.5	−0.4	0	—	—
6	−1.4	1.2	−11.6	0	−0.9	0	−7.7	13.6	−9.9	4.4	—	—
7	−0.7	1.0	—	—	−1.2	0	−8.7	11.1	−0.3	0	—	—
8	−0.9	0	−13.7	0	−3.3	0.3	—	—	−5.4	0	—	—
9	−1.1	1.6	−9.6	0	−1.5	0	−5.1	8.6	−0.8	0	−7.5	0